Stem Cell Reports

Article

Cell-Type-Specific Adhesiveness and Proliferation Propensity on Laminin Isoforms Enable Purification of iPSC-Derived Corneal Epithelium

Shun Shibata,[1,2] Ryuhei Hayashi,[1,3,*] Yuji Kudo,[1,2] Toru Okubo,[1,2] Tsutomu Imaizumi,[1,2] Tomohiko Katayama,[3] Yuki Ishikawa,[3] Yuki Kobayashi,[3] Junko Toga,[4] Yukimasa Taniguchi,[4] Yoichi Honma,[1,2] Kiyotoshi Sekiguchi,[4] and Kohji Nishida[3,5]

[1]Department of Stem Cells and Applied Medicine, Osaka University Graduate School of Medicine, Suita, Osaka 565-0871, Japan
[2]Research and Development Division, ROHTO Pharmaceutical Co., Ltd., Osaka, Osaka 544-8666, Japan
[3]Department of Ophthalmology, Osaka University Graduate School of Medicine, Suita, Osaka 565-0871, Japan
[4]Division of Matrixome Research and Application, Institute for Protein Research, Osaka University, Suita, Osaka 565-0871, Japan
[5]Integrated Frontier Research for Medical Science Division, Institute for Open and Transdisciplinary Research Initiatives (OTRI), Osaka University, Suita, Osaka 565-0871, Japan
*Correspondence: ryuhei.hayashi@ophthal.med.osaka-u.ac.jp
https://doi.org/10.1016/j.stemcr.2020.02.008

SUMMARY

A treatment for intractable diseases is expected to be the replacement of damaged tissues with products from human induced pluripotent stem cells (hiPSCs). Target cell purification is a critical step for realizing hiPSC-based therapy. Here, we found that hiPSC-derived ocular cell types exhibited unique adhesion specificities and growth characteristics on distinct E8 fragments of laminin isoforms (LNE8s): hiPSC-derived corneal epithelial cells (iCECs) and other non-CECs rapidly adhered preferentially to LN332/411/511E8 and LN211E8, respectively, through differential expression of laminin-binding integrins. Furthermore, LN332E8 promoted epithelial cell proliferation but not that of the other eye-related cells, leading to non-CEC elimination by cell competition. Combining these features with magnetic sorting, highly pure iCEC sheets were fabricated. Thus, we established a simple method for isolating iCECs from various hiPSC-derived cells without using fluorescence-activated cell sorting. This study will facilitate efficient manufacture of iCEC sheets for corneal disease treatment and provide insights into target cell-specific scaffold selection.

INTRODUCTION

Regenerative medicine employing human pluripotent stem cells (hPSCs), such as human embryonic stem cells (hESCs) and human induced pluripotent stem cells (hiPSCs) holds considerable potential for the treatment of diverse diseases (Takahashi et al., 2007; Thomson et al., 1998; Yu et al., 2007).

The use of hPSCs has attracted considerable attention in the treatment of visual impairment. The cornea is located on the outermost surface of the eye and is a transparent tissue through which light passes. Damage to corneal epithelial (CE) stem cells leads to invasion of the conjunctiva with blood vessels to the center of the eyes, which results in blindness (Daniels et al., 2001; Shapiro et al., 1981). We previously generated hiPSC-derived structures—named SEAMs (self-formed ectodermal autonomous multi-zones)—that mimic eye development; SEAMs contain various eye-related cells and the CE primordium, which can be isolated using fluorescence-activated cell sorting (FACS) and can form functional cell sheets that are therapeutically effective in an experimentally induced animal model of corneal blindness (Hayashi et al., 2016). Therefore, hiPSC-derived corneal epithelial cell (iCEC) sheet transplantation is expected to serve as a strategy for replacing the damaged corneal epithelium in severe corneal disease.

For culturing hPSCs, the heterotrimeric basement membrane protein laminin and its short fragments (LNE8s) are widely used (Miyazaki et al., 2012; Rodin et al., 2010; Xu et al., 2001); laminin is composed of α, β, and γ chains and is the binding partner of integrin. Intriguingly, laminin isoforms, named by combinations of α, β, and γ chains (Aumailley et al., 2005), were recently found to largely affect ocular cell differentiation from hiPSCs (Shibata et al., 2018).

Here, we examined the use of laminin isoforms for purifying iCECs and manufacturing iCEC sheets for hiPSC-based corneal therapy. We found that iCECs exhibited cell-type-specific adhesiveness and proliferation propensity on laminin isoforms, and exploitation of these properties in combination with magnetic cell sorting (MACS) (Miltenyi et al., 1990) enabled iCEC isolation without using FACS.

RESULTS

Cell-Type-Specific Adhesion to Laminin Isoforms

We first examined the adhesiveness of iCECs to E8 fragments of laminin isoforms. After ocular cell differentiation, the differentiated cells were seeded onto dishes coated with five types of LNE8 (111, 211, 332, 411, and 511); 10–20 min later, non-adherent cells were collected and analyzed using flow cytometry (Figure 1A). iCECs (SSEA-4^{+}/ITGB4^{+}/CD200^{−}) were markedly diminished among non-adherent cells from LN332/411/511E8-coated
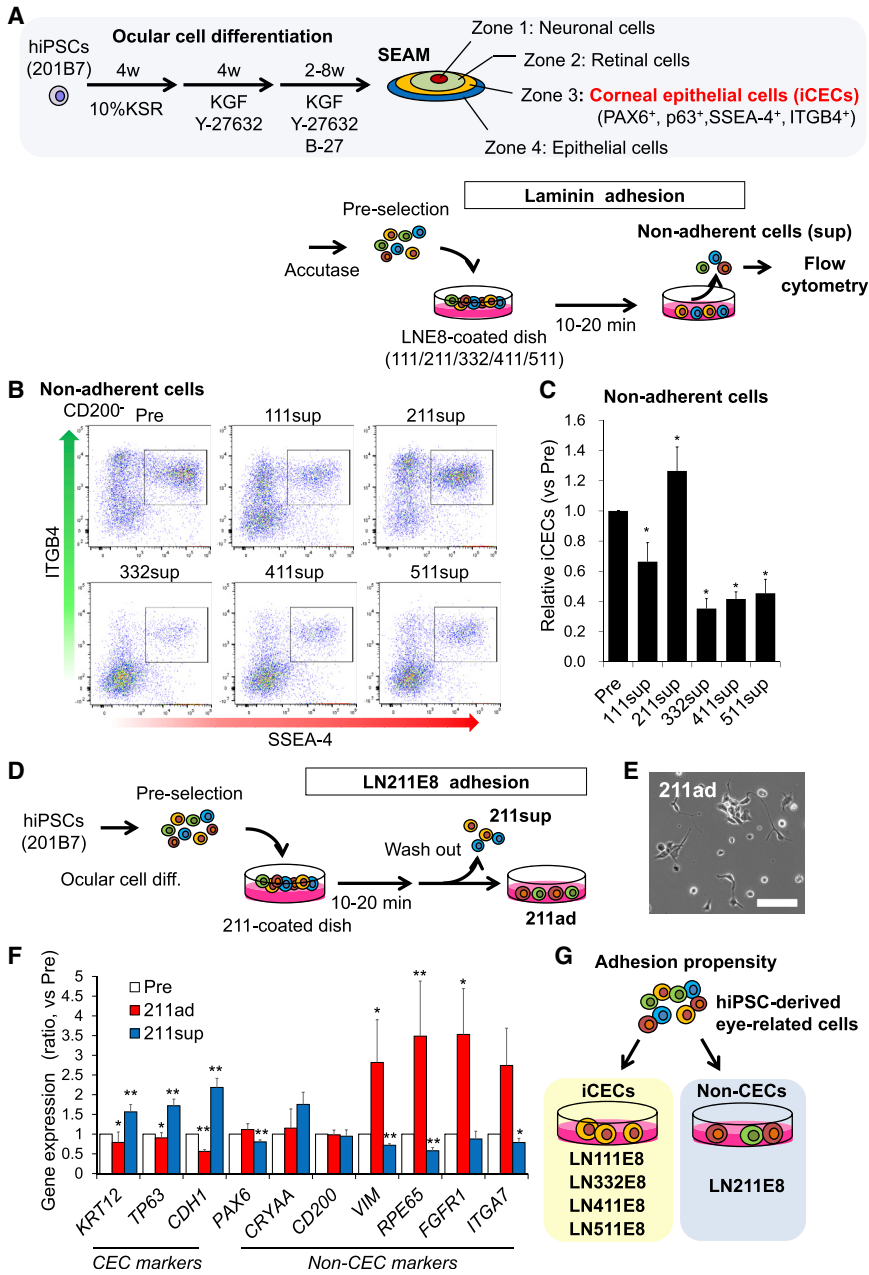
Figure 1. Adhesiveness of hiPSC-Derived Cells to Laminin Isoforms

(A) Schematic of differentiation and experimental method.

(B and C) Flow cytometry analysis for iCECs among non-adherent cells on each LNE8 (B). Relative iCECs (SSEA-4$^+$/ITGB4$^+$/CD200$^-$ vs Pre-selection) among non-adherent cells. n = five independent experiments; *$p < 0.05$ (C).

(D) Schematic of experimental method.

(E) Phase contrast image of iPSC-derived eye-related cell attached to LN211E8. Scale bar, 100 μm.

(F) Gene expression analysis for markers related to CECs and non-CECs in the population of LN211E8-adherent cells. n = six independent experiments; *$p < 0.05$, **$p < 0.01$.

(G) Schematic of adhesion propensity exhibited toward laminin isoforms.

See also Figure S1.

dishes (Figures 1B and 1C), which suggested that iCECs rapidly adhered specifically to LN332/411/511E8. Separate analysis of SSEA-4$^+$/CD200$^-$ and ITGB4$^+$/CD200$^-$ cells revealed that ITGB4$^+$/CD200$^-$ cells exhibited stronger selective adhesion to LN332/411/511E8 (Figure S1). Conversely, the iCEC fraction among non-adherent cells seeded on LN211E8 increased as compared with the cells before seeding. Thus, we hypothesized that LN211E8 possesses the ability to specifically adsorb cells other than iCECs. To test this, differentiated cells were seeded on

LN211E8 and non-adherent cells were washed out after a 10- to 20-min incubation (Figure 1D). Gene expression analysis was then performed. As compared with pre-seeding cells, LN211E8-adherent cells showed spindle cell shapes (Figure 1E), lower expression of CEC-marker genes, such as *KRT12*, *TP63*, and *CDH1*, and higher expression of non-CEC genes, such as *VIM*, *RPE65*, *FGFR1*, and *ITGA7* (Figure 1F). These results showed that iCECs and non-CECs display adhesiveness to LN332/411/511E8 and LN211E8, respectively (Figure 1G).

Differential Expression of Laminin-Binding Integrins and the Adhesion of Epithelial and Non-epithelial Cells to Distinct Laminin Isoforms

To investigate the differences in adhesion by cell type, we isolated the cells in each zone (1, 2, and 3/4) of SEAM by manual pipetting (Figure 2A). As previously reported, even after reseeding with single cells, the cells in zone 1 were positive for neuronal markers, including TUBB3 and those in zone 2 were positive for retinal markers, including VSX2. Zone 3/4 cells were epithelial cells expressing E-cadherin and P63 (Figures 2B and S2A). Furthermore, we separately examined the rapid adhesion of non-epithelial and epithelial cells to LNE8s. Non-epithelial cells adhered to all LNE8s (211, 332, and 511) at a constant rate. However, epithelial cells effectively adhered to LN332E8 and LN511E8, but hardly adhered to LN211E8 (Figures 2C and 2D). Thereafter, we examined the expression levels of laminin-binding integrins in cells in each zone of SEAM. Epithelial cells (zone 3/4 of SEAM) highly expressed laminin-binding integrin genes, including *ITGA3* and *ITGA6*, along with *ITGB1* and *ITGB4*, relative to those in non-epithelial cells (zones 1 and 2). Conversely, *ITGA7*, an LN211 receptor, was highly expressed in non-epithelial cells than in epithelial cells (Figure 2E). We further examined the protein expression of laminin-binding integrins. Consistent with the results of gene expression analysis, ITGA3, ITGA6, ITGB1, and ITGB4 were upregulated in epithelial cells (zone 3/4), and the proportion of cells expressing these integrins was also considerably higher in epithelial cells. Furthermore, the proportion of both epithelial cells and non-epithelial cells expressing ITGA7 was low (Figures 2F, 2G, and S2B). Moreover, we examined the expression of ITGB4, a laminin-binding integrin with marked differential expression between epithelial cells and non-epithelial cells, in adherent epithelial cells by immunostaining. Interestingly, the few epithelial cells adhering to LN211E8 were ITGB4$^-$, whereas several ITGB1$^+$ cells were present. However, most epithelial cells adhering to LN332/511E8 expressed ITGB4 (Figure 2H). Furthermore, treatment with an ITGB4-neutralizing antibody of epithelial cells inhibited their adhesion to LN332/511E8 but not to LN211E8 (Figure 2I). Non-epithelial cells (ITGB4$^-$) adhering to all LNE8s were positive for other laminin-binding integrins, including ITGA6, ITGA7, and ITGB1 (Figure S2C). Moreover, treatment with an ITGA6-neutralizing antibody inhibited the adhesion of non-epithelial cells to all LNE8s (Figure S2D). These results suggest that epithelial cells rich in laminin-binding integrins are more efficient in adhering to LN332E8 and LN511E8 than non-epithelial cells and that LN211E8 has a low adsorptive effect on ITGB4$^+$ cells localized in zone 3/4 of SEAM (Figure 2J).

Distinct Proliferation Propensities of SEAM-Derived Cells on Different Laminin Isoforms

Recapitulating the *in vivo* environment in *in vitro* cultures is critical. Therefore, we analyzed the expression of laminin isoforms in the mouse cornea at embryonic day (E18.5), which is equivalent to the developmental stage of the CE primordium in the SEAM after 10–15 weeks of differentiation (Hayashi et al., 2016). Immunohistochemical staining results showed that Lama3 and Lama5 were expressed in the CE basement membrane (Figure 3A). We determined which cell type in the SEAM is likely to increase on which laminin isoform: iCECs (SSEA-4$^+$/ITGB4$^+$/CD200$^-$) and the cells in zone 4 (SSEA-4$^-$/ITGB4$^+$/CD200$^-$), i.e., epithelial cells other than corneal cells, were isolated using FACS, and the other eye-related cells (in zones 1 and 2) were isolated through manual pipetting from SEAMs; these cells were cultured on distinct laminin isoforms (Figure 3B). On seeding iCECs, LN332E8 and LN511E8, both of which were also expressed in the CE *in vivo*, effectively promoted iCEC proliferation. However, the adhesion efficiency of iCEC was poor, and the cells proliferated as colonies on LN111E8, LN211E8, and LN411E8 (Figures 3C and 3D). The number of other epithelial cells (zone 4) was also high on LN332E8 or LN511E8. By contrast, the cells in zones 1 and 2 did not appear to increase readily on LN332E8 (Figure 3E). Moreover, differentiation of the zone 1 cells into cells of various neuroectodermal lineages was suppressed on LN332E8 (Figure S3A); similarly, neuroepithelial spheres did not proliferate efficiently on LN332E8 (Figures S3B–S3D).

These results suggest that there are different proliferation propensities in each eye-related cell type on distinct laminin isoforms, and that on LN332E8, epithelial cells and the other eye-related cells are relatively more and less likely, respectively, to proliferate (Figure 3F).

LN332E8 as a Substrate Promoting Elimination of Non-CECs in Cell Competition

In previous reports, to fabricate iCEC sheets, iCECs (SSEA-4$^+$/ITGB4$^+$ cells) were sorted by FACS and seeded onto LN511E8-coated dishes (Hayashi et al., 2017). Moreover, non-CEC colonies can sometimes be formed on iCEC sheets (Hayashi et al., 2018). Based on the results that iCECs easily proliferate and non-CECs hardly increase on LN332E8, we hypothesized that LN332E8 is an optimal substrate for iCEC sheet fabrication without contaminating non-CECs. iCECs and non-CECs were intentionally mixed in a 10:1 ratio, and then seeded on five types of LNE8, after which they were cultured (Figure 4A). Similar to the results in Figure 3, iCEC proliferation was positively observed during the growth process, especially on LN332E8 (Figure 4B). Consequently, non-CEC colonies were divided into small areas. Intriguingly, time-lapse
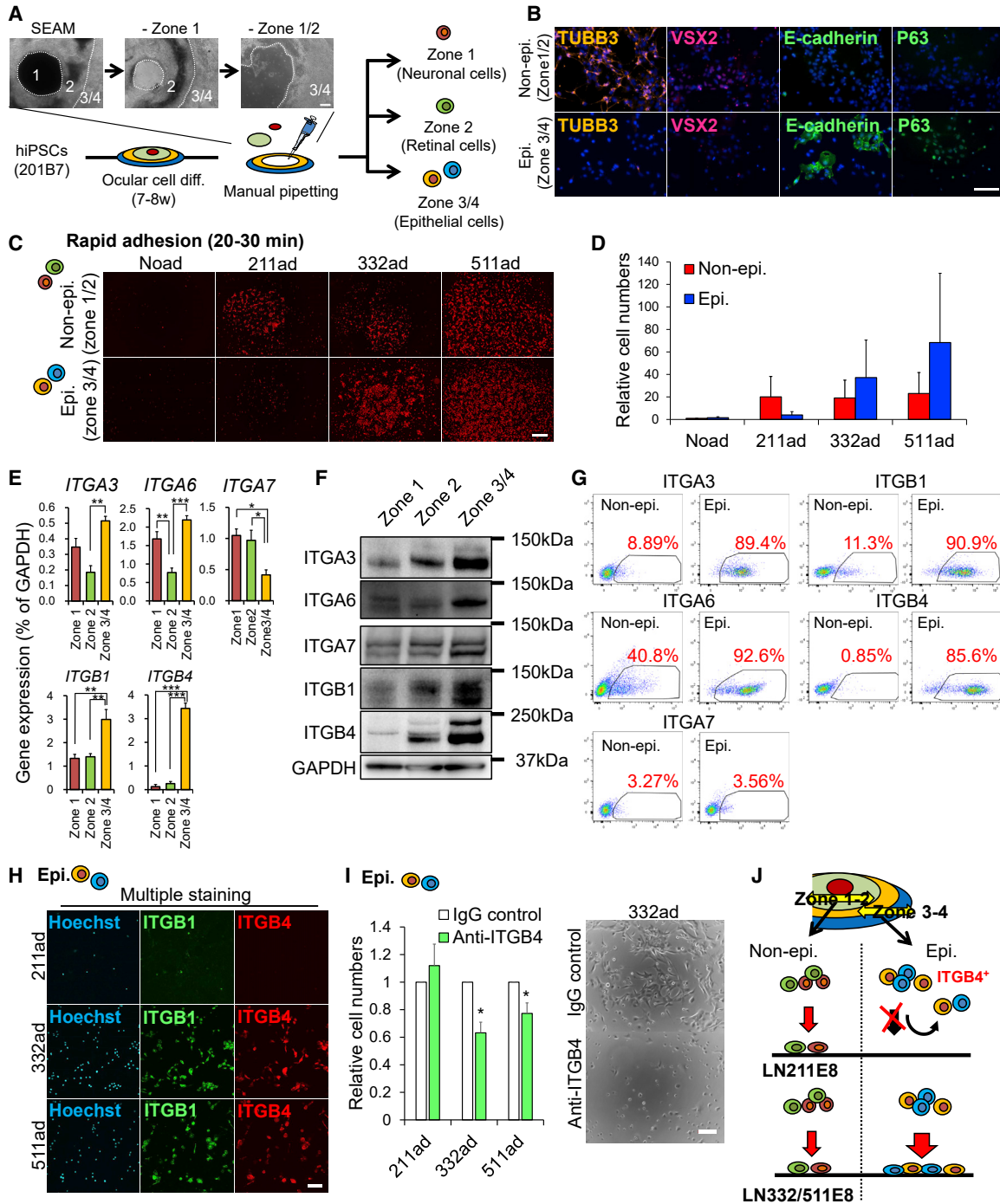
Figure 2. Differential Integrin Expression and Adhesion Properties to Laminins in Epithelial and Non-epithelial Cells

(A) Schematic of experimental method and phase contrast images of cells during manual pipetting. Scale bar, 200 μm.

(B) Immunostaining for TUBB3 (orange), VSX2 (red), E-cadherin (green), and P63 (green) in non-epithelial cells (zone 1/2) and epithelial cells (zone 3/4); nuclei, blue. Scale bar, 100 μm.

(C) Hoechst staining (red) in adhered cells. Scale bar, 500 μm. Noad, cells adhered to no coated dishes.

(D) Relative adhered cell numbers (vs non-epithelial cells of Noad). n = six independent experiments. Noad, cells adhered to no coated dishes.

(legend continued on next page)

observation revealed that cell competition occurred with the exclusion of non-CEC colonies by the proliferation of surrounding iCECs on LN332E8 (Figure 4C; Video S1). After 3–4 weeks of culture, the entire culture well was scanned to quantify the area of non-CEC colonies. It was quantitatively revealed that non-CEC colonies were excluded on LN332E8 as compared with the other types of LNE8s. Conversely, the area of non-CECs was the larger on LN111E8 and LN211E8 (Figures 4D and 4E). Similarly, gene expression levels of non-CEC markers in mixed cells were the lower on LN332E8 (Figure 4F). These results showed that LN332E8, which increases iCECs but not non-CECs, promotes the elimination of non-CECs from iCEC sheet.

Enrichment of Epithelial Stem Cells by MACS and Subsequent Specific and Rapid Adhesion to LNE8s

We next examined whether MACS, a high-throughput method (10^{11} cells/h; FACS, 10^7 cells/h) (Nicodemou and Danisovic, 2017), can be used for iCEC isolation instead of FACS. After ocular cell differentiation for 10–15 weeks, we performed MACS, which comprised removal of CD200^{+} cells followed by positive selection for SSEA-4^{+} cells (Figure 5A). Gene expression levels of the CEC markers *KRT12*, *PAX6*, and *TP63* were increased and those of non-CEC markers were decreased after MACS (CD200^{−}/SSEA-4^{+}) (Figure 5B). We also analyzed the cells at each stage of MACS by using flow cytometry to quantify the iCEC fraction (i.e., the fraction of CD200^{−}/SSEA-4^{+}/ITGB4^{+} cells). The MACS process (CD200^{−}/SSEA-4^{+}) enriched the iCEC fraction from 16.8% to 68.6% (Figures 5C and 5D). However, non-CECs still remained (31.4%) after MACS (CD200^{−}/SSEA-4^{+}), which suggested that the MACS process alone was insufficient for the purification.

Next, we determined whether adhesiveness to laminin isoforms could be used to enrich epithelial stem cells, similar to ITGB4^{+} selection, which is not performed in MACS. Previously, we established a knockin (KI) hiPSC line in which the expression of the epithelial stem cell marker P63 can be visualized based on the fluorescence of enhanced green fluorescent protein (EGFP) (Kobayashi et al., 2017). The KI-P63 hiPSCs were differentiated into ocular cells and used for evaluating isolation accuracy. CD200^{−}/SSEA-4^{+} cells were concentrated by MACS and subsequent laminin adhesion steps, which consisted of adsorption on LN332/511E8 isoforms (expressed in the CE *in vivo*) after adsorption based on LN211E8 adhesion (Figure 5E). Among the cells that rapidly adhered to LN211E8 after MACS, the proportion of P63^{+} cells was 36%. When the LN211 non-adherent cells (211sup) were seeded onto LN332/511E8, the proportion was 67.9% and 60.0%. Furthermore, the proportions of P63^{+} cells were increased when the non-adherent cells on LN332/511E8 were washed out 10–20 min after seeding (85.9% and 78.9%, Figures 5F and 5G). These results showed that epithelial stem cells adhered specifically to LN332/511E8 in a short time. The finding suggests that iCECs can be enriched by combining MACS (CD200^{−}/SSEA-4^{+}) with subsequent adsorption of non-target cells and epithelial stem cells on LN211E8 and LN332/511E8, respectively.

Preparation of High-Purity hiCEC Sheets Using MACS Followed by LN211E8 and LN332E8 Adhesion and Culturing

Finally, to fabricate hiCEC sheets, we used—based on the results obtained thus far—a method combining MACS and LN211/332E8 adhesion (Figure 6A). Sorted cells (M+2sup/3ad) showed uniform cobblestone-like morphology and grew to confluence (Figure 6B; Video S2). Conversely, the cells adsorbed on LN211E8 after MACS (M+2ad) showed CD200^{+} and non-epithelial morphologies (Figure 6C). This indicates that residual CD200^{+} cells after MACS can be depleted through adsorption by LN211E8. Consistent with results of Figure 4, time-lapse microscopy revealed that even when a few impurities were mixed with iCECs, they were eliminated, and this led to the formation of pure iCEC sheets on LN332E8 (Figures S4A–S4C).

We also evaluated the quality of the cell sheets. The cells prepared using our method were positive for CEC markers, such as PAX6, KRT14, and KRT12 across the sheets (Figure 6D). When LN511E8 was used instead of LN332E8, colonies of non-CEC colonies formed occasionally (Figure S4D). Flow cytometry analysis of the cell sheets

(E) Gene expression analysis for laminin-binding integrins in cells in zone 1, zone 2, and zone 3/4 of SEAMs. n = four independent experiments; *p < 0.05, **p < 0.01, ***p < 0.001.
(F) Western blotting for laminin-binding integrins and GAPDH (loading control) in cells in zones 1, 2, and 3/4 of SEAMs.
(G) Flow cytometry analysis for laminin-binding integrins in non-epithelial and epithelial cells. Representative results are presented from two or three independent experiments.
(H) Immunostaining for ITGB1 (green) and ITGB4 (red) in adhered cells; nuclei, blue. Scale bar, 100 μm.
(I) Relative numbers of adhered cells with anti-ITGB4 antibodies or IgG control. n = three independent experiments. *p < 0.05 (left). Phase contrast images of adhered cells with antibodies on LN332E8. Scale bar, 100 μm (right).
(J) Schematic of cell-type-specific integrin expression and adhesiveness to laminins.
See also Figure S2.
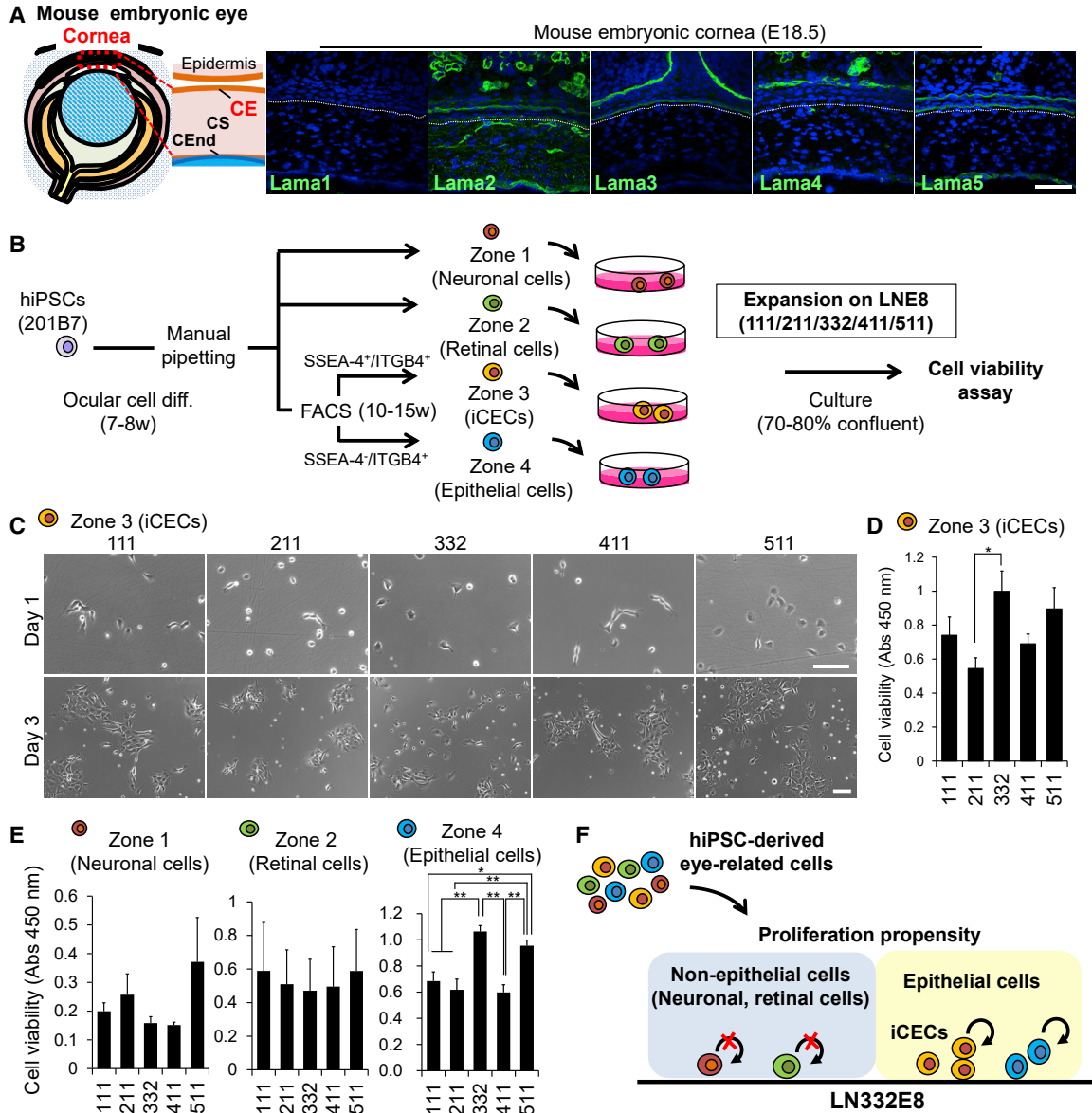
Figure 3. Cell-Type-Specific Proliferation Propensity on Each LNE8

(A) Schematic of mouse embryonic eye (left). Immunostaining for Lama1–5 (green) in mouse embryonic eye at E18.5 (right); nuclei, blue. Scale bar, 100 μm.

(B) Schematic of experimental method.

(C) Phase contrast images of iCECs on LNE8s at day 1 (upper) and day 3 (lower). Scale bars, 100 μm.

(D) Cell viabilities of iCECs on LNE8s. n = five independent experiments. *p < 0.05.

(E) Cell viabilities of zones 1, 2, and 3/4 of SEAMs on LNE8s. n > three independent experiments. *p < 0.01, **p < 0.01.

(F) Schematic of each cell proliferation propensity on LN332E8.

See also Figure S3.

revealed that the proportion of the iCEC fraction (SSEA-4$^+$/ITGB4$^+$/CD200$^-$ cells) was very high (98.6%, Figure 6E), and that the expression of the mature CE marker KRT12 was sufficiently high (69.1%, Figure 6F). We also confirmed that the iCEC sheets were properly stratified and expressed CE markers, such as KRT12, P63, PAX6, and MUC16 (Figures 6G and 6H).

Thus, highly pure iCEC sheets could be prepared by combining MACS with LN211/332E8-adhesion steps without using FACS.
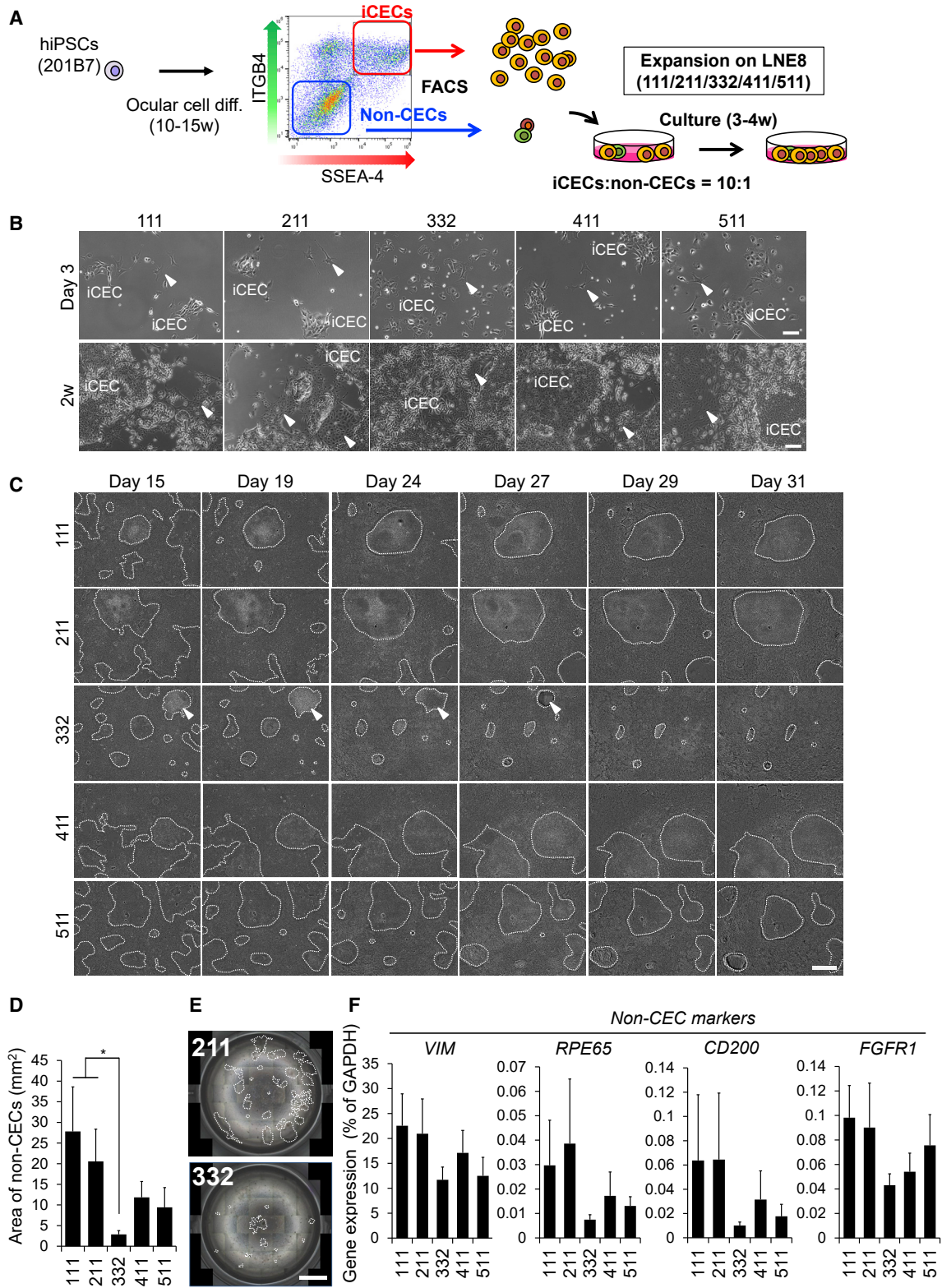
(legend on next page)

DISCUSSION

Transplantation of iCEC sheets holds considerable potential as a strategy for treating CE diseases, and for treatment efficacy, effective purification of hiCEC sheets is critical. Here, we established a simple method for iCEC purification by exploiting cell-type-specific adhesion and proliferation on laminin isoforms.

We found that distinct eye-related cells exhibit divergent adhesiveness to E8 fragments of laminin isoforms: iCECs, particularly CD200⁻/ITGB4⁺ cells, adhered to LN332/411/511E8 but did not readily adhere to LN211E8 in a short time, whereas non-CECs in SEAMs preferentially bound to LN211E8. Consistently, cells expressing non-CE-marker genes, such as *VIM*, *RPE65*, *FGFR1*, and *ITGA7*, rapidly adhered to LN211E8 (Figure 1). Furthermore, by analyzing non-epithelial cells (zone 1/2 in SEAM) and epithelial cells (zone 3/4 in SEAM) separately by manual pipetting, we found that non-epithelial cells adhere to LN211/332/511E8, whereas epithelial cells (zone 3/4 in SEAM) efficiently adhere to LN332/511E8 but not to LN211E8 (Figures 2C and 2D). Laminins show various binding specificities for integrin, with each laminin isoform differentially binding to distinct integrin subunits (Nishiuchi et al., 2006; Yamada and Sekiguchi, 2015). Therefore, to elucidate the mechanism underlying cell-type-specific adhesion to various laminins, it is important to understand the expression of laminin-binding integrins in each cell type. We analyzed the expression of laminin-binding integrins in each zone. In epithelial cells, the expression of laminin-binding integrins except, ITGA7, was higher than that in non-epithelial cells. Epithelial stem cells, including corneal limbal epithelial stem cells, can be isolated as cells that rapidly adhere to basement membrane proteins that are used as a scaffold *in vivo* (Dunnwald et al., 2001; Igarashi et al., 2008; Jones and Watt, 1993; Li et al., 2005; Strachan et al., 2008). These rapidly adherent cells show high expression of integrin β1 or α6 (Hayashi et al., 2008; Jones and Watt, 1993; Kim et al., 2004). iCECs are also defined as ITGB4⁺ (and SSEA-4⁺) cells (Hayashi et al., 2016). We also confirmed that iCECs and other epithelial cells (correspond to zone3/4) highly expressed *ITGA3*, *ITGA6*, *ITGB1*, and *ITGB4* (Figures 2E–2G). Thus,

epithelial stem/progenitor cells showing high expression of laminin-binding integrins, such as α3β1, α6β1, and α6β4 are likely to adhere rapidly to the extracellular matrix, such as laminins (-332 or -511), which are coated experimentally or secreted by the cells themselves. However, non-epithelial cells adhered to LN211E8, whereas epithelial cells only slightly adhered to LN211E8. Laminin α2 (component of LN211) is recognized to bind integrin α7 (Yamada and Sekiguchi, 2015), which is predominantly expressed in muscle cells, peripheral nerve cells, and other cells (Colognato and Yurchenco, 2000). Consistently, gene expression level of *ITGA7* was high in non-epithelial cells as compared with that in epithelial cells (Figure 2E). However, at the protein level, ITGA7 expression in non-epithelial cells was equivalent to that in epithelial cells, and the proportion of ITGA7-positive cells was low in both non-epithelial cells (2.78%) and epithelial cells (3.35%) (Figures 2F and 2G). Therefore, the difference in epithelial and non-epithelial adhesion to LN211E8 may not be explained on the basis of ITGA7 expression. Laminin α2 (component of LN211) is also known not to bind integrin β4 (Yamada and Sekiguchi, 2015). Consistent with that report, most of the cells adhering to LN211E8 were ITGB4⁻, and the inhibition experiments with neutralizing antibodies revealed that ITGB4 was not utilized for their attachment to LN211E8 (Figures 2H and 2I). This suggested that ITGB4⁺ cells do not adhere to LN211E8. However, ITGB4⁻ non-epithelial cells also adhere to LN211E8 through other integrins, such as α6β1 (Figures S2C and S2D). Thus, prior to the isolation of iCECs, it is appropriate to use LN211E8, as it facilitates the adsorption of ITGB4⁻ non-epithelial cells. This leads to the accumulation of ITGB4⁺ cells in the supernatant, which did not adhere after seeding on LN211E8.

We also found that hiPSC-derived cells showed cell-type-specific proliferation propensity on each LNE8. The expression of laminin α3 (a component of LN332) was detected in the basement membrane of stratified epithelial cells, epidermis, and CE *in vivo* (Figure 3A). Moreover, data for immunohistological staining of laminins in mouse basement membrane during development can be obtained from the Mouse Basement Membrane Bodymap (http://dbarchive.biosciencedbc.jp/archive/matrixome/bm/home.html).

Figure 4. Cell Competition between iCECs and Non-iCECs on Different Laminin Isoforms

(A) Schematic of experimental method.

(B) Phase contrast images of cells mixed with iCECs and non-CECs at a ratio of 10:1 at day 3 (upper) and week 2 (lower). Scale bars, 100 μm. Arrowheads indicate non-CECs.

(C) Time-lapse images of cells mixed with iCECs and non-CECs at a ratio of 10:1 during culture. Displayed non-CEC colonies are surrounded by dashed lines. Scale bar, 800 μm. Arrowheads indicate non-CEC colony that are gradually eliminated on LN332E8.

(D) Total area of non-CECs in mixed cells per well of 12-well plate. n = seven independent experiments. *p < 0.05.

(E) Scanning the entire well of the 12-well plate. Displayed non-CEC colonies are surrounded by dashed lines. Scale bar, 5 mm.

(F) Gene expression analysis for non-CEC markers in mixed cells. n = seven independent experiments.

A

hiPSCs (201B7) → **Pre-MACS** → CD200 depletion → SSEA-4 positive selection → CD200⁻/SSEA-4⁺

Ocular cell diff.

CD200⁻

MACS

B

KRT12, TP63, PAX6, CRYAA, RPE65, CD200

Gene expression (ratio, vs Pre)

(Pre, CD200-, CD200-/SSEA-4+)

C

MACS — Pre / CD200⁻ / CD200⁻/SSEA-4⁺

CD200 / CD200⁻ / ITGB4 / SSEA-4

D

Proportion of cells (%)

iCEC / Non-CEC

Pre, CD200-, CD200-/SSEA-4+

E

P63 EGFP → hiPSCs (1383D2) (EGFP-P63) → Ocular cell diff. → CD200⁻/SSEA-4⁺ → 211sup → 211ad → 332/511-coated dish → 10-20 min → Wash out (or not) → 332/511ad

MACS   Laminin adhesion

F

211sup: 211ad, 332, 332ad, 511, 511ad

EGFP (P63) / Phase

G

EGFP (P63)-positive cells (%)

211ad, 332, 332ad, 511, 511ad

211sup

*** ** * *

(legend on next page)

The limited use of laminin α3 in developmental eye *in vivo* was mirrored by the proliferative activity observed *in vitro*: on LN332E8, only epithelial cells were found to be likely to increase, and the other non-target cells, such as neurons and retinal cells (corresponding to zones 1 and 2, respectively), were less likely to increase (Figures 3D and 3E).

Furthermore, we found that the outcome of cell competition between iCECs and non-CECs was altered by the affinity of the cells for distinct laminins and the growth characteristics. Epithelial cells maintain a constant number by pushing cells out of the dense area (Eisenhoffer et al., 2012). The rate of this cell extrusion is controlled by cell growth and density (Marinari et al., 2012). Such cell competition occurs between cells having dissimilar gene expression or mechanical properties, and is involved in the maintenance of homeostasis, tumor suppression, and development (Bras-Pereira and Moreno, 2018; Maruyama and Fujita, 2017; Sancho et al., 2013). The tumor suppression mechanism by epithelial cells, not mediated by immune cells, is named epithelial defense against cancer as the cytoskeletal proteins filamin and vimentin accumulate at the cell-cell interface and generate a contractile force that can exclude transformed cells (Kajita et al., 2014). Although little is known about the role of substrates in cell competition, a recent report showed that stem cell competition contributes to the maintenance of skin homeostasis, the mechanism of which is mediated by the expression levels of collagen 17A1 in epidermal stem cells (Liu et al., 2019). Thus, affinity of the cells for the scaffold might largely affect cell competition. Further studies are needed to determine the molecules that play a role in the cell competition among different cell types. In this study, we showed that cell-type specific adhesion and growth properties on distinct laminin isoforms affected the outcome of cell competition during iCEC sheet formation. In particular, LN332E8 promoted the elimination of non-CECs (Figure 4). By controlling which of the different cell types will be the "winner" during competition by a specific laminin, it would be possible to ensure cell purity for regenerative medicine.

We ultimately established an isolation method that involves concentration of the iCEC fraction using MACS (CD200$^-$/SSEA-4$^+$) plus a dual laminin adhesion step:

removal of non-CECs by adhesion on LN211E8 and adsorption of iCECs on LN332E8. We first used CD200, a negative marker for iCECs that we reported as suitable for depletion (Hayashi et al., 2018), and then performed positive selection for SSEA-4 on CD200$^-$ cells. In the case of MACS, co-positive cells were not obtained. Therefore, among the two positive markers, we selected SSEA-4, which is relatively more specific for the CE primordium in hiPSC-derived SEAMs. Although MACS effectively concentrated the iCEC fraction, the purity of iCECs was not sufficiently high after MACS (CD200$^-$/SSEA-4$^+$) because ITGB4-based selection was not performed. Laminin 332 is known to bind to ITGB4 (Yamada and Sekiguchi, 2015) and its adsorption to LN332E8 is a step that corresponds to the enrichment of ITGB4$^+$ cells, which could not be performed in the MACS process. By using the KI cell line in which P63 expression can be visualized based on EGFP fluorescence (Kobayashi et al., 2017), we confirmed that the cells that did not bind to LN211E8 but bound to LN332E8 rapidly were strongly P63$^+$ (Figure 5). These multiple steps and subsequent CE maintenance culture enabled highly pure iCEC sheets to be obtained (Figure 6). The method established in this study is simple and can be readily disseminated; moreover, the method can be scaled-up using MACS with high throughput.

When iCEC (SSEA-4$^+$/ITGB4$^+$) fraction was sorted by FACS, after seeding iCECs into culture plates, several non-CEC colonies were occasionally obtained in iCEC sheets (Hayashi et al., 2018). We also found that in our established method, accidentally contaminating non-CEC colonies were eliminated by the surrounding iCECs, which suggests that even if impurities are present, they can be eliminated due to the proliferation capacity of iCECs. Therefore, a culture environment that promotes CEC proliferation, which affects purity, is critical. Accordingly, in addition to LN332E8 as suitable substrate, we used a CE maintenance medium containing keratinocyte growth factor and a Rho kinase inhibitor, which is suitable for CEC culture (Miyashita et al., 2013).

This is the report of the use of cell-type-specific properties on the E8 fragments of laminin isoforms for both adsorption of non-target cells and enrichment of target cells. We also showed that the affinity to the scaffold changes the outcome of cell competition among different cell types, and that it

Figure 5. Concentration of Epithelial Stem Cells by Using MACS and Laminin Adhesion
(A) Schematic of experimental method.
(B) Relative gene expression levels of CEC- and non-CEC-related markers in cells from each step of MACS. n = four independent experiments.
(C) Flow cytometry analysis for SSEA-4$^+$/ITGB4$^+$/CD200$^-$ cells in each step of MACS.
(D) Quantification of iCECs and other non-CECs among the cells from each step of MACS. n = three independent experiments.
(E) Schematic of experimental method.
(F) Fluorescence and phase contrast images of EGFP/P63 (green) in hiPSC-derived cells attached to specific LNE8s. Scale bar, 50 μm. The arrows indicate P63$^-$ cells.
(G) Quantification of P63$^+$ cells (EGFP) among adherent cells. n = four independent experiments. *p < 0.05, **p < 0.01, ***p < 0.001.
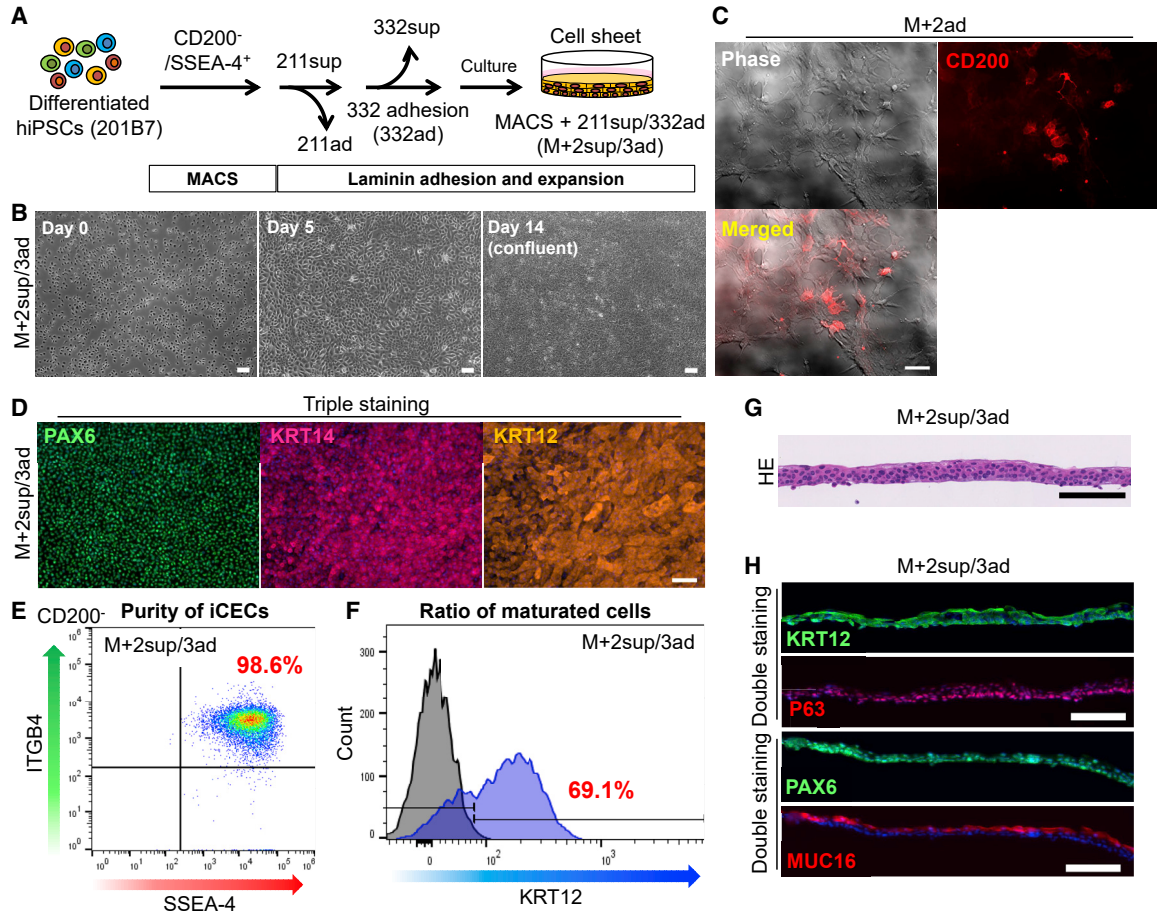
Figure 6. Preparation of High-Purity hiCEC Sheets by Using MACS Followed by Laminin Adhesion Steps

(A) Schematic of experimental method.

(B) Phase contrast images of isolated cells (M+2sup/3ad). Scale bars, 100 μm.

(C) Phase contrast and fluorescence images (CD200, red) of cells adhered to LN211E8 after MACS (M+2ad). Scale bar, 100 μm.

(D) Immunostaining for PAX6 (green), KRT14 (red), and KRT12 (orange) in iCEC sheets prepared using the established method (M+2sup/3ad). Scale bar, 100 μm.

(E and F) Flow cytometry analysis for SSEA-4^{+}/ITGB4^{+}/CD200^{−} cells (E) and KRT12^{+} cells (F) in iCEC sheets prepared using the established method (M+2sup/3ad). Results are presented as means of two independent experiments.

(G and H) H&E staining (G) and immunostaining for KRT12 (green), P63 (red), PAX6 (green), and MUC16 (red) (H) in iCEC sheets prepared using the M+2sup/3ad method; nuclei, blue. Scale bars, 100 μm (G and H).

See also Figure S4.

has a potential for application to the purification of cells in regenerative medicine. Both MACS and LNE8-based purification could be readily adapted for use in Good Manufacturing Practice compliant procedures. This method enables efficient and scalable manufacture of iCEC sheets for the treatment of intractable corneal diseases.

EXPERIMENTAL PROCEDURES

hiPSC Culture

hiPSC line 201B7 was provided by the RIKEN BioResource Center (Tsukuba, Japan). hiPSC line 1383D2 was obtained from the Center

for iPS Cell Research and Application (Kyoto University). We also used the KI P63-EGFP hiPSC line that we previously established (Kobayashi et al., 2017). hiPSCs were cultured on LN511E8 (0.5 μg cm^{-2}, iMatrix-511, Nippi, Tokyo, Japan), together with StemFit medium (Ajinomoto, Tokyo, Japan) in a humidified 5% CO_2/95% air atmosphere at 37°C. All experiments involving the use of recombinant DNA were approved by and conducted according to the regulations of the Recombinant DNA Committees of Osaka University.

Laminin Coating

Culture plates were coated with recombinant LNE8 fragments by adding phosphate-buffered saline (PBS) to the plates and then

adding LNE8 fragments at a density of 0.5–1.0 μg cm^{-2}. Plates were incubated at 37°C for at least 1 h.

Ocular Cell Differentiation

hiPSC differentiation into the SEAM was induced using a protocol based on previous reports (Hayashi et al., 2016, 2017). hiPSCs were seeded onto dishes coated with LN332/511E8 and cultured in StemFit medium for 10 days; subsequently, the medium was switched to differentiation medium; 4 weeks later, the medium was replaced with corneal differentiation medium and the cells were cultured for an additional 4 weeks. At the beginning of week 9, the medium was replaced with CE maintenance medium, in which the cells were cultured for 2–8 weeks.

Flow Cytometry

Cells were dissociated using Accutase (Life Technologies, Carlsbad, CA) or Accumax (Innovative Cell Technologies, San Diego, CA) and stained with antibodies (Table S1) for 30–60 min on ice. A FACSVerse (BD Biosciences) or SH800 (Sony, Tokyo, Japan) system was used for the analysis, and cell sorting was performed using an SH800 device. Compensation was performed using single color-stained controls and gating was performed based on isotype-negative controls (Table S1). Data analysis were performed by using Sony SH800 and FlowJo software (TreeStar, San Carlos, CA).

Quantitative Real-Time Reverse Transcription PCR

Total RNA was isolated from cells by using QIAzol reagent (QIAGEN, Venlo, Netherlands), and cDNA was synthesized using a SuperScript III First-Strand Synthesis System for qRT-PCR (Life Technologies). qRT-PCR was performed using an ABI Prism 7500 Fast Sequence Detection System (Life Technologies). TaqMan probes used were described in Table S2.

Immunofluorescence Staining

Cells were fixed in 4% paraformaldehyde, washed thrice in Tris-buffered saline (TBS). For blocking, the cells were incubated in TBS containing 5% donkey serum and 0.3% Triton X-100 for 1 h. Next, the cells were incubated with primary antibodies (Table S1) overnight at 4°C and then stained with Alexa Fluor-conjugated secondary antibodies (Life Technologies) and Hoechst 33342. Stained cells were examined using Axio Observer D1 (Carl Zeiss, Germany).

Western Blotting

Cell lysis were prepared with RIPA buffer (25 mM Tris-HCl [pH 7.6], 150 mM NaCl, 1% NP-40, 1% sodium deoxycholate, 0.1% SDS; Thermo Fisher Scientific, Waltham, MA) containing protease inhibitor cocktail (Wako, Osaka, Japan) and PhosSTOP (Roche, Penzberg, Upper Bavaria, Germany). Protein concentration was determined using a Pierce BCA Protein Assay Kit (Thermo Fisher Scientific). SDS-PAGE were conducted using NuPAGE 4%–12% gradient Bis-Tris gels and proteins were transferred to polyvinylidene fluoride membranes using an iBlot system (Invitrogen). The membranes were incubated with antibodies against primary antibodies (Table S1) for overnight at 4°C. After washing, they were incubated with secondary antibodies for 1 h at room temperature.

Proteins were detected with ECL Prime (GE Healthcare, Pittsburgh, PA) and scanned with a ChemiDoc XRS+ imaging system (Bio-Rad, Hercules, CA).

Adhesion Assay

Non-epithelial cells and epithelial cells were isolated from differentiated iPSCs through manual pipetting. The cells were dissociated using Accutase (Life Technologies) or Accumax and filtered through a 40-μm nylon mesh filter (BD Falcon). The cells (50,000 cells/well) were seeded onto LNE8-coated 96-well plates (Coastar). After incubation for 10–20 min at 37°C, non-adherent cells were washed out with DMEM/F-12 twice. CE maintenance medium was then supplemented. The adherent cells were fixed with 4% paraformaldehyde, washed thrice with TBS, and stained with Hoechst 33342. Stained nuclei were imaged and quantified using a BZ-X810 microscope (Keyence, Osaka, Japan).

Immunohistochemical Analyses

Pregnant female mice (C57/BL6; 10–16 weeks old; E18.5) were acquired from SLC Japan (Shizuoka, Japan) for analysis of embryonic eyes. Frozen tissues obtained at E18.5 were sectioned, air-dried, and incubated for 1 h with TBS (TaKaRa Bio, Shiga, Japan) containing 5% donkey serum and 0.3% Triton X-100 (Sigma-Aldrich, St. Louis, MO). Next, the sections were incubated with primary rat antibodies specific to laminin isoform (Manabe et al., 2008) overnight at 4°C, and then with Alexa Fluor-conjugated secondary antibodies (Life Technologies) and Hoechst 33342 stain (Wako, no. 346-07951). Stained samples were examined using LSM710 (Carl Zeiss) microscopes. Animal experimentation was approved by the animal ethics committee of Osaka University.

Cell Viability Assay

Cell viability assay was performed by using the Cell Counting Kit-8 (Dojindo, Kumamoto, Japan), according to the manufacturer's instructions.

Quantification of Area of Non-CECs

iCECs (SSEA-4$^+$/ITGB4$^+$/CD200$^-$) and non-CECs (SSEA-4$^+$/ITGB4$^-$) were sorted by FACS. These cells were mixed at a ratio of 10:1 and seeded onto five types of LNE8s (0.5 μg cm^{-2}), followed by culturing for 3–4 weeks with CE maintenance medium. The non-CEC colonies on each LNE8 were manually enclosed and the total area of non-CEC colonies per well was calculated using EVOS FL Auto microscope and the accompanying software (Life Technologies).

MACS

For CD200 depletion, the cells were dissociated using Accutase (Life Technologies) and stained with PE-Cy7-conjugated CD200 antibody (624052, BD Biosciences) for 30 min on ice. Subsequently, the cells were washed with MACS buffer (PBS containing 2 mM EDTA and 0.5% BSA) and labeled with Anti-Cy7 MicroBeads (no. 130-091-652, Miltenyi Biotec, Germany) for 15 min at 4°C. After labeling, the cells were applied onto the MS column of a Mini-MACS or the LD column of a MidiMACS magnetic-separation kit (Miltenyi Biotec), and the unlabeled cells that passed through

were collected and subject to SSEA-4^{+} selection: The CD200^{+} cell-depleted fractions were labeled with Anti-SSEA-4 MicroBeads (no. 130-097-855, Miltenyi Biotec) for 10 min at 4°C and, after washing with MACS buffer, were applied to the MS or LS column. The labeled cells were collected as post-MACS cells.

Quantification of EGFP-Positive (P63[+]) Cells

Phase contrast and fluorescence images of five different areas were randomly acquired using an Axio Observer D1 microscope, and the EGFP/P63^{+} cells among all the cells were counted and their ratio was calculated. For the counting, we used the cell-counter plug-in of ImageJ program.

Harvesting and Assessment of iCEC Sheets

For harvesting, iCEC sheets were treated with 2.4 U mL^{-1} dispase (Life Technologies) at 37°C for 10 min. For immunostaining, iCEC sheets were embedded in Tissue-Tek O.C.T. Compound (Sakura Finetek, Tokyo, Japan) and frozen. For hematoxylin and eosin (H&E) staining, iCEC sheets were fixed with 10% formalin (Nacalai Tesque, Kyoto, Japan), washed with distilled water, embedded in paraffin, and sectioned at a thickness of 3 μm. After deparaffinization and hydration, the sections were stained with H&E and examined using a NanoZoomer-XR C12000 (Hamamatsu Photonics, Hamamatsu, Japan) and an Axio Observer D1.

Time-Lapse Imaging

Time-lapse imaging was conducted using an IncuCyte Live-Cell Imaging System (ESSEN BioScience, Ann Arbor, MI).

Statistical Analysis

Statistical significance was analyzed via Steel, Tukey-Kramer, Mann-Whitney, and Steel-Dwass tests using StatLight 2000 software (Yukms, Tokyo, Japan). All statistical analyses were conducted with a significance level of α = 0.05 ($p < 0.05$). All data are represented as the mean ± standard error.

SUPPLEMENTAL INFORMATION

Supplemental Information can be found online at https://doi.org/10.1016/j.stemcr.2020.02.008.

AUTHOR CONTRIBUTIONS

S.S., R.H., K.S., and K.N. designed the research. S.S., Y. Kudo, T.O., T.I., T.K., Y.I., and Y. Kobayashi. performed the experiments and analyzed the data. J.T., Y.T., and K.S. prepared and provided reagents (LNE8s and anti-mouse laminin α antibodies). Y.H., K.S., and K.N. supervised the project. S.S. and R.H. analyzed the data and wrote the paper.

ACKNOWLEDGMENTS

REFERENCES

Aumailley, M., Bruckner-Tuderman, L., Carter, W.G., Deutzmann, R., Edgar, D., Ekblom, P., Engel, J., Engvall, E., Hohenester, E., Jones, J.C., et al. (2005). A simplified laminin nomenclature. Matrix Biol. *24*, 326–332.

Bras-Pereira, C., and Moreno, E. (2018). Mechanical cell competition. Curr. Opin. Cell Biol. *51*, 15–21.

Colognato, H., and Yurchenco, P.D. (2000). Form and function: the laminin family of heterotrimers. Dev. Dyn. *218*, 213–234.

Daniels, J.T., Dart, J.K., Tuft, S.J., and Khaw, P.T. (2001). Corneal stem cells in review. Wound Repair Regen. *9*, 483–494.

Dunnwald, M., Tomanek-Chalkley, A., Alexandrunas, D., Fishbaugh, J., and Bickenbach, J.R. (2001). Isolating a pure population of epidermal stem cells for use in tissue engineering. Exp. Dermatol. *10*, 45–54.

Eisenhoffer, G.T., Loftus, P.D., Yoshigi, M., Otsuna, H., Chien, C.B., Morcos, P.A., and Rosenblatt, J. (2012). Crowding induces live cell extrusion to maintain homeostatic cell numbers in epithelia. Nature *484*, 546–549.

Hayashi, R., Yamato, M., Saito, T., Oshima, T., Okano, T., Tano, Y., and Nishida, K. (2008). Enrichment of corneal epithelial stem/progenitor cells using cell surface markers, integrin alpha6 and CD71. Biochem. Biophys. Res. Commun. *367*, 256–263.

Hayashi, R., Ishikawa, Y., Sasamoto, Y., Katori, R., Nomura, N., Ichikawa, T., Araki, S., Soma, T., Kawasaki, S., Sekiguchi, K., et al. (2016). Co-ordinated ocular development from human iPS cells and recovery of corneal function. Nature *531*, 376–380.

Hayashi, R., Ishikawa, Y., Katori, R., Sasamoto, Y., Taniwaki, Y., Takayanagi, H., Tsujikawa, M., Sekiguchi, K., Quantock, A.J., and Nishida, K. (2017). Coordinated generation of multiple ocular-like cell lineages and fabrication of functional corneal epithelial cell sheets from human iPS cells. Nat. Protoc. *12*, 683–696.

Hayashi, R., Ishikawa, Y., Katayama, T., Quantock, A.J., and Nishida, K. (2018). CD200 facilitates the isolation of corneal epithelial cells derived from human pluripotent stem cells. Sci. Rep. *8*, 16550.

Igarashi, T., Shimmura, S., Yoshida, S., Tonogi, M., Shinozaki, N., and Yamane, G.Y. (2008). Isolation of oral epithelial progenitors using collagen IV. Oral Dis. *14*, 413–418.

Jones, P.H., and Watt, F.M. (1993). Separation of human epidermal stem cells from transit amplifying cells on the basis of differences in integrin function and expression. Cell *73*, 713–724.

Kajita, M., Sugimura, K., Ohoka, A., Burden, J., Suganuma, H., Ikegawa, M., Shimada, T., Kitamura, T., Shindoh, M., Ishikawa, S., et al. (2014). Filamin acts as a key regulator in epithelial defence against transformed cells. Nat. Commun. *5*, 4428.

Kim, D.S., Cho, H.J., Choi, H.R., Kwon, S.B., and Park, K.C. (2004). Isolation of human epidermal stem cells by adherence and the reconstruction of skin equivalents. Cell. Mol. Life Sci. *61*, 2774–2781.

Kobayashi, Y., Hayashi, R., Quantock, A.J., and Nishida, K. (2017). Generation of a TALEN-mediated, p63 knock-in in human induced pluripotent stem cells. Stem Cell Res. *25*, 256–265.

Li, D.Q., Chen, Z., Song, X.J., de Paiva, C.S., Kim, H.S., and Pflugfelder, S.C. (2005). Partial enrichment of a population of human limbal epithelial cells with putative stem cell properties based on collagen type IV adhesiveness. Exp. Eye Res. *80*, 581–590.

Liu, N., Matsumura, H., Kato, T., Ichinose, S., Takada, A., Namiki, T., Asakawa, K., Morinaga, H., Mohri, Y., De Arcangelis, A., et al. (2019). Stem cell competition orchestrates skin homeostasis and ageing. Nature *568*, 344–350.

Manabe, R., Tsutsui, K., Yamada, T., Kimura, M., Nakano, I., Shimono, C., Sanzen, N., Furutani, Y., Fukuda, T., Oguri, Y., et al. (2008). Transcriptome-based systematic identification of extracellular matrix proteins. Proc. Natl. Acad. Sci. U S A *105*, 12849–12854.

Marinari, E., Mehonic, A., Curran, S., Gale, J., Duke, T., and Baum, B. (2012). Live-cell delamination counterbalances epithelial growth to limit tissue overcrowding. Nature *484*, 542–545.

Maruyama, T., and Fujita, Y. (2017). Cell competition in mammals - novel homeostatic machinery for embryonic development and cancer prevention. Curr. Opin. Cell Biol. *48*, 106–112.

Miltenyi, S., Muller, W., Weichel, W., and Radbruch, A. (1990). High gradient magnetic cell separation with MACS. Cytometry *11*, 231–238.

Miyashita, H., Yokoo, S., Yoshida, S., Kawakita, T., Yamagami, S., Tsubota, K., and Shimmura, S. (2013). Long-term maintenance of limbal epithelial progenitor cells using rho kinase inhibitor and keratinocyte growth factor. Stem Cells Transl. Med. *2*, 758–765.

Miyazaki, T., Futaki, S., Suemori, H., Taniguchi, Y., Yamada, M., Kawasaki, M., Hayashi, M., Kumagai, H., Nakatsuji, N., Sekiguchi, K., et al. (2012). Laminin E8 fragments support efficient adhesion and expansion of dissociated human pluripotent stem cells. Nat. Commun. *3*, 1236.

Nicodemou, A., and Danisovic, L. (2017). Mesenchymal stromal/stem cell separation methods: concise review. Cell Tissue Bank *18*, 443–460.

Nishiuchi, R., Takagi, J., Hayashi, M., Ido, H., Yagi, Y., Sanzen, N., Tsuji, T., Yamada, M., and Sekiguchi, K. (2006). Ligand-binding specificities of laminin-binding integrins: a comprehensive survey of laminin-integrin interactions using recombinant alpha3beta1, alpha6beta1, alpha7beta1 and alpha6beta4 integrins. Matrix Biol. *25*, 189–197.

Rodin, S., Domogatskaya, A., Ström, S., Hansson, E.M., Chien, K.R., Inzunza, J., Hovatta, O., and Tryggvason, K. (2010). Long-term self-renewal of human pluripotent stem cells on human recombinant laminin-511. Nat. Biotechnol. *28*, 611–615.

Sancho, M., Di-Gregorio, A., George, N., Pozzi, S., Sanchez, J.M., Pernaute, B., and Rodriguez, T.A. (2013). Competitive interactions eliminate unfit embryonic stem cells at the onset of differentiation. Dev. Cell *26*, 19–30.

Shapiro, M.S., Friend, J., and Thoft, R.A. (1981). Corneal re-epithelialization from the conjunctiva. Invest. Ophthalmol. Vis. Sci. *21*, 135–142.

Shibata, S., Hayashi, R., Okubo, T., Kudo, Y., Katayama, T., Ishikawa, Y., Toga, J., Yagi, E., Honma, Y., Quantock, A.J., et al. (2018). Selective laminin-directed differentiation of human induced pluripotent stem cells into distinct ocular lineages. Cell Rep. *25*, 1668–1679.e5.

Strachan, L.R., Scalapino, K.J., Lawrence, H.J., and Ghadially, R. (2008). Rapid adhesion to collagen isolates murine keratinocytes with limited long-term repopulating ability in vivo despite high clonogenicity in vitro. Stem Cells *26*, 235–243.

Takahashi, K., Tanabe, K., Ohnuki, M., Narita, M., Ichisaka, T., Tomoda, K., and Yamanaka, S. (2007). Induction of pluripotent stem cells from adult human fibroblasts by defined factors. Cell *131*, 861–872.

Thomson, J.A., Itskovitz-Eldor, J., Shapiro, S.S., Waknitz, M.A., Swiergiel, J.J., Marshall, V.S., and Jones, J.M. (1998). Embryonic stem cell lines derived from human blastocysts. Science *282*, 1145–1147.

Xu, C., Inokuma, M.S., Denham, J., Golds, K., Kundu, P., Gold, J.D., and Carpenter, M.K. (2001). Feeder-free growth of undifferentiated human embryonic stem cells. Nat. Biotechnol. *19*, 971–974.

Yamada, M., and Sekiguchi, K. (2015). Molecular basis of laminin-integrin interactions. Curr. Top. Membr. *76*, 197–229.

Yu, J., Vodyanik, M.A., Smuga-Otto, K., Antosiewicz-Bourget, J., Frane, J.L., Tian, S., Nie, J., Jonsdottir, G.A., Ruotti, V., Stewart, R., et al. (2007). Induced pluripotent stem cell lines derived from human somatic cells. Science *318*, 1917–1920.